Fibers and Polymers 2016, Vol.17, No.12, 2124-2130
DOI 10.1007/s12221-016-6271-8

ISSN 1229-9197 (print version)
ISSN 1875-0052 (electronic version)

Symmetrical Napcore and Honeycomb Sandwich Structures under Impact Load

Nils Gerber*, Christoph Uhlig, Christian Dreyer, and Yvonne Chowdhury[1]

Research Division Polymeric Materials and Composites PYCO, Fraunhofer-Institute for Applied Polymer Research IAP, Teltow 14513, Germany
[1]*InnoMat GmbH, Teltow 14513, Germany*

(Received February 26, 2016; Revised October 2, 2016; Accepted October 10, 2016)

Abstract: Sandwich structures are state of the art for construction of lightweight structures with high mechanical load capacity. Beside established core materials like foams, honeycombs or wood, napcore material is an interesting option when economic production costs or the possibility to integrate extra functionality are criteria in addition to specified mechanical values. Napcore material is made from a two-dimensional resin-impregnated knitted fabric that is shaped into a three-dimensional nap structure and stabilized by the cured resin matrix. In this paper the mechanical behavior under low velocity impact loads of sandwich structures made with napcores from aramide textile and phenolic resin is investigated and compared with components containing honeycomb cores.

Keywords: Textile, Napcore, Composite, Impact, Honeycomb

Introduction

Most lining elements for aircraft cabins are based on sandwich panels made from phenolic resin impregnated glass fiber top layers and honeycomb cores [1]. Due to their excellent mechanical properties and high fire retardancy Nomex® Honeycombs are extensively used in aircraft sandwich structures [2]. With its hexagonal cells this core material supports the face sheets in the shape of a coherent grid and offers high specific strength and stiffness [3]. Disadvantages of the material are the price intensive production process, its limited drapability, and the closed cell structure when face sheets are applied, which can result in inclusion and accumulation of condensation water, resulting in a weight increase and reduction of mechanical properties [4,5].

In contrast to honeycombs, napcores are made from a two-dimensional fabric that is formed and stabilized in a three-dimensional shape. Napcores offer less strength than a honeycomb with similar density, but on the other hand they show a number of advantageous properties like the possibility to integrate functionalities [1]. Beside a better drapability the open structure of this core material allows to drain or to vent the panel and to integrate cables, tubes, and wires into the sandwich [6]. The possibility to use different fiber materials, knitting techniques, matrix polymers, and various nap geometries results in a wide range of properties and offers excellent adaptability to numerous applications. Knitted fabrics made from thermoplastic polymers, aramide, glass, cellulose, basalt and hybrid fibers were processed to napcore material successfully so far.

Initially napcores were made from thermoplastic materials as described in patent CA1016716 A from 1977 [7]. Disselbeck and Stahl invented napcores made from a resin impregnated fabric, stabilized by the cured resin matrix in 1986 [8]. Due to their unique characteristics that set them apart from other core materials like foams, honeycombs or wood, napcores with thermoset resin matrix were subject of further research [9,10]. Although napcores were mechanically characterized in static tests [11,12] research on impact behavior is not reported so far. Due to the curved structure of the symmetrical napcores and the support of the face sheets by unconnected circular areas the assumption was made that sandwich panels from napcore material dissipate punctual loads better and are less sensitive to impact stress than honeycomb sandwiches.

This paper presents an experimental investigation of the low velocity impact behavior under different impact energies in the range from 3 J to 7 J. Composite sandwich structures with napcore made from aramide textile and phenolic resin are tested and compared to sandwich structures with a hexagonal honeycomb core. Generally, impact can be categorized into low velocity impact, medium velocity impact and high velocity impact but these categories are not clearly separated from each other and authors disagree on their definition. Sjöblom et al. define low-velocity impact as quasi-static where the upper limit for the impact speed can vary from one to tens of m/s in dependence on the target stiffness [13]. Cantwell and Morton classified low velocity up to 10 m/s [14]. Having impact speeds from 1.21 m/s up to 1.91 m/s, the experiments in the present paper can be classified as low velocity impact.

Experimental

Two types of sandwich structures were tested. Sandwiches with a honeycomb, type C2-3,2-48 from Schuetz GmbH & Co. KGaA were manufactured as reference. The Nomex®

*Corresponding author: nils.gerber@iap.fraunhofer.de

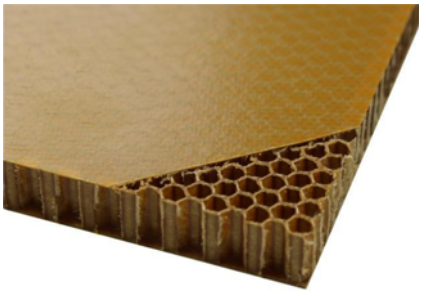

Figure 1. Sandwich panel with honeycomb core.

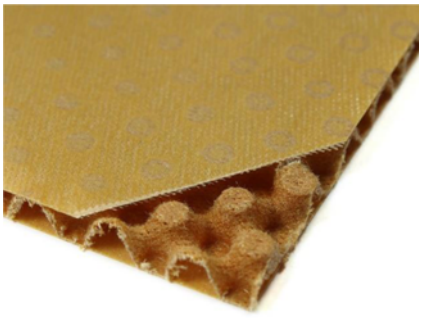

Figure 2. Sandwich panel with symmetrical napcore.

honeycomb with a cell width of 3.2 mm and a density of 48 kg/m^3 exhibits a compressive strength of 2.0 MPa. The 8 mm thick core material was combined with face sheets from Isovolta Airpreg PC 8242. The phenolic resin prepreg consists of a glass fabric with a surface weight of 296 g/m^2 and an 8H satin weave pattern. The total prepreg weight is 521 g/m^2, corresponding to a resin content of 42.7 %. The reference sandwich is shown in Figure 1.

The symmetrical napcore sandwiches were made from a knitted fabric (80 % aramide; 20 % polyester) with a surface weight of 165 g/m^2. Phenolic resin Eponol 0639 V C2 from Momentive was used to impregnate the fabric resulting in a resin content of 50±3 %. The final core material has a density of approximately 53 kg/m^3 and a compressive strength of 0.73 MPa. The selected geometry has naps with a diameter of 6 mm and a nap-distance of 12 mm. Identically as for the honeycombs the symmetrical napcore with a thickness of 8 mm was combined with face sheets from Isovolta Airpreg PC 8242 (see Figure 2).

Both components were manufactured using a vacuum bagging process at 0.4 bar in a convection oven at 135 °C, 75 minutes with a 5 min. heating ramp.

The low velocity impact tests were performed on an IM10 Drop Weight Impact Tester from Imatek Ltd. equipped with an impactor of 16 mm diameter shown in Figure 3(a). The instrumented Impact Tester is able to measure both load and displacement during the impact. The sandwich plates of 120 mm×120 mm used for the impact testing were fixed on a support-frame with a circular cutout with 75 mm diameter.

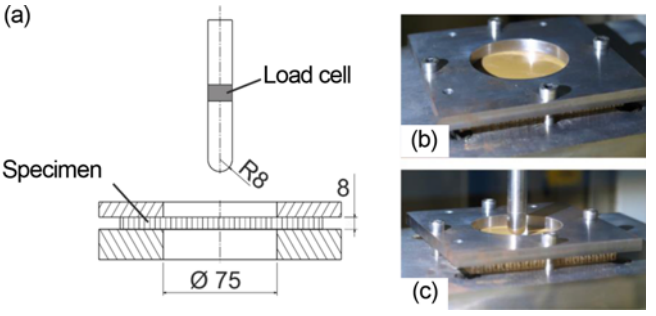

Figure 3. Setup for impact tests; (a) side view of the setup, (b) fixation of the sandwich panel, and (c) sandwich panel with impactor.

Table 1. Pre-set impact energies, measured impact energies and impact speed for napcore sandwiches

Sample	Pre-set impact energy (J)	Measured impact energy (J)	Impact speed (m/s)
NC 3J-1/2/3	3	2.65/2.66/2.68	1.23/1.23/1.23
NC 4J-1/2/3	4	3.67/3.60/3.61	1.44/1.43/1.43
NC 5J-1/2/3	5	4.52/4.52/4.59	1.60/1.60/1.61
NC 6J-1/2/3	6	5.52/5.50/5.51	1.77/1.77/1.77
NC 7J-1/2/3	7	6.40/6.40/6.43	1.90/1.90/1.91
NC 8J-1/2/3	8	7.30/7.40/7.39	2.03/2.05/2.0

Table 2. Pre-set impact energies, measured impact energies and impact speed for honeycomb sandwiches

Sample	Pre-set impact energy (J)	Measured impact energy (J)	Impact speed (m/s)
HC 3J-1/2/3	3	2.64/2.67/2.67	1.22/1.23/1.23
HC 4J-1/2/3	4	3.61/3.59/3.64	1.43/1.43/1.44
HC 5J-1/2/3	5	4.57/4.51/4.61	1.61/1.60/1.62
HC 6J-1/2/3	6	5.54/5.52/5.52	1.77/1.77/1.75
HC 7J-1/2/3	7	6.42/6.42/6.43	1.91/1.91/1.91

An impactor with a mass of 3.53 kg was used to apply impact energies between 2.64 and 7.4 J by increasing the drop height respectively. Due to friction during the drop of the impactor the measured impact energy is lower than the pre-set value. Both values are listed in Tables 1 and 2.

For each impact energy a set of three samples was tested. To visualize the damage and to measure the deformation of the surfaces one sample from each set was scanned additionally with an ATOS 3D-Scanner.

Results and Discussion

Depending on the drop height, the impact results in a more or less distinct deformation of the sandwich structure. Schubel *et al.* [15] identified four different failure modes for impact damage on foam core sandwich panels. These are

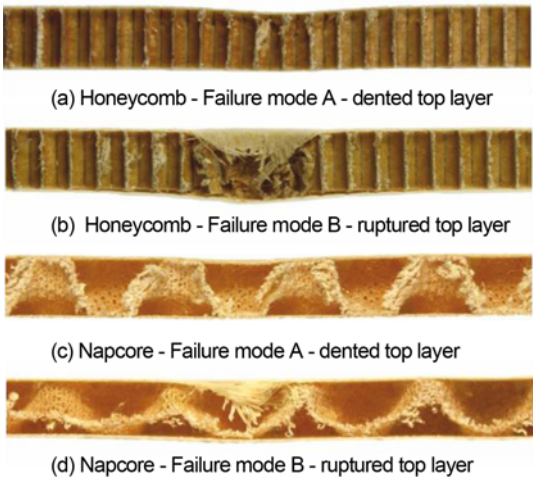

Figure 4. Honeycomb samples with the two different failure modes after impact with pre-set energies of 4 J (a) and 7 J (b) Napcore samples with the two different failure modes after impact with pre-set energies of 4 J (c) and 8 J (d).

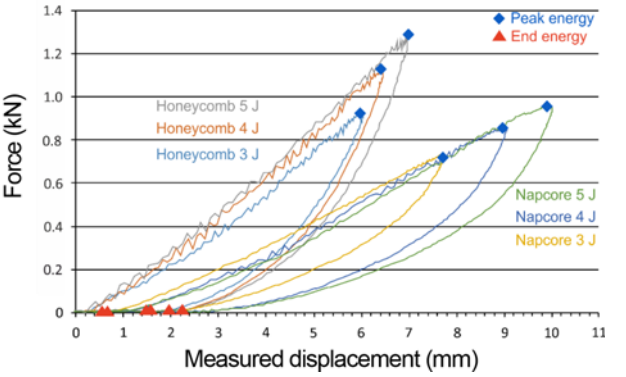

Figure 5. Force vs. measured displacement for honeycomb and napcore sandwiches for pre-set impact energies of 3 J, 4 J and 5 J (in all cases failure mode A).

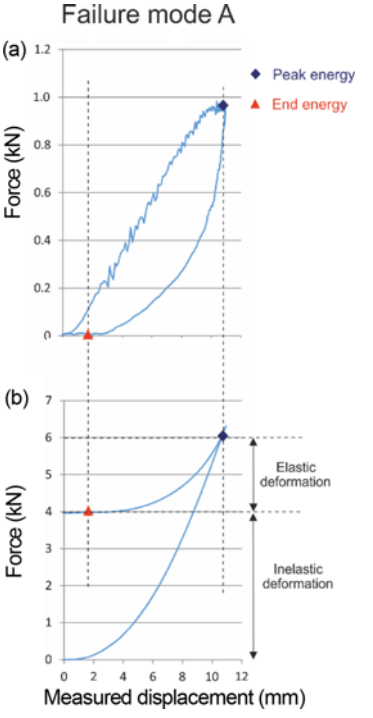

Figure 6. (a) Force vs. measured displacement for napcore sandwich for pre-set impact energy of 7 J and (b) energy vs. measured displacement for napcore sandwich for pre-set impact energy of 7 J.

delamination in the face sheet, matrix cracking and fiber breakage, debond at the face-core interface and core crushing (permanent deformation) in the region surrounding the point of impact. For the tested samples delamination of the face sheet is not relevant as the face sheet consists of a single layer. The damage mechanisms of honeycomb and napcore should differ significantly from those of foam.

For the tested sandwiches two failure modes are defined in this paper. Low impact energies (3 J, 4 J) damage mainly the top layer causing an indentation on the surface of the sandwich panel which is defined as failure mode A. For higher impact energies the failure is characterized by rupturing of the top layer, which is defined as failure mode B. The difference between both failure modes is illustrated in Figure 4.

For failure mode A with a dented top layer both sandwiches show a similar force progression in dependence of the measured displacement. Figure 5 illustrates the force-displacement curves for napcore and honeycomb sandwiches for pre-set impact energies of 3 J, 4 J and 5 J.

All samples show a hysteresis which is evidence for a partly elastic deformation. The steeper force progression of the honeycomb samples indicates a higher stiffness of the core material compared to the napcore structure. For comparable impact energies the impactor is decelerated more by the honeycomb structure which results in a higher peak force and a significantly lower deformation compared to the napcore structure.

The hexagonal structure of the honeycomb core not only results in a higher stiffness but also limits the tolerable impact energy before passing to failure mode B which is characterized by the rupture of the top layer. As soon as the impactor penetrates the sandwich structure the deformation is fully irreversible. Figure 7 shows the energy progression of both failure modes for pre-set impact energies of 7 J. The proportion of elastic and inelastic deformation can be determined by comparison of peak energy and end energy. The peak energy describes the energy level at maximum force, whereas the end energy equates the energy level after the force decreased to zero again. For failure mode A the peak energy is higher than the end energy, whereas it is

lower than the end energy for failure mode B.

The progression curve of the energy can be divided into two sections for each failure mode. Failure mode A is illustrated in Figure 6. Characteristic for an elastic deformation the energy curve increases parabolically to the peak energy where the measured displacement reaches its maximum. Afterwards the sandwich structure resiliences and the curve decreases in a similar parabolic way with reduced slope to the level of end energy. The difference between peak energy and end energy is equivalent to the elastic deformation of the sandwich structure, whereas the end energy correlates to the ineleastic deformation.

The progression curve changes completely for failure mode B when the top layer is ruptured (see Figure 7). In this case the energy curve increases parabolically as well to the peak energy but after the rupture of the top layer the impactor penetrates the sandwich structure. This is visible by the approximately linear section of the curve above this point (see Figure 7(b)), which is characteristic for an inelastic deformation. The curve increases to a peak caused by the bottom layer, but does not decrease significantly anymore in contrast to failure mode A which means that no energy retrieved by resilience.

As mentioned above the napcore geometry tolerates

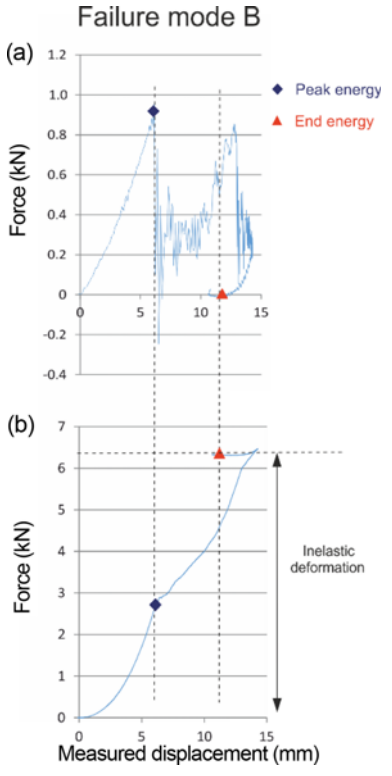

Figure 7. (a) Force vs. measured displacement for honeycomb sandwich for pre-set impact energy of 7 J and (b) energy vs. measured displacement for honeycomb sandwich for pre-set impact energy of 7 J.

Table 3. Peak energies and end energies for napcore sandwiches

Sample	Peak energy (J)	End energy (J)
NC 3J - 1/2/3	2.77/2.75/2.74	1.23/1.26/1.25
NC 4J - 1/2/3	3.68/3.65/3.71	1.87/1.65/1.81
NC 5J - 1/2/3	4.55/4.53/4.67	2.33/2.37/2.51
NC 6J - 1/2/3	5.54/5.51/5.55	3.39/2.99/3.15
NC 7J - 1/2/3	6.17/6.27/6.44	3.98/4.57/3.83
NC 8J - 1/2*/3*	7.05/5.95/6.11	4.87/6.50/6.45

*Failure mode B with ruptured face sheet.

Table 4. Peak energies and end energies for honeycomb sandwiches

Sample	Peak energy (J)	End energy (J)
HC 3J - 1/2/3	2.73/2.72/2.78	1.44/1.44/1.36
HC 4J - 1/2/3	3.66/3.63/3.67	2.03/1.95/1.95
HC 5J - 1/2*/3*	4.58/3.71/2.88	2.50/4.34/4.21
HC 6J - 1*/2*/3*	2.06/1.93/3.43	5.85/5.95/5.56
HC 7J - 1*/2*/3*	2.63/2.80/3.69	6.36/6.09/6.03

*Failure mode B with ruptured face sheet.

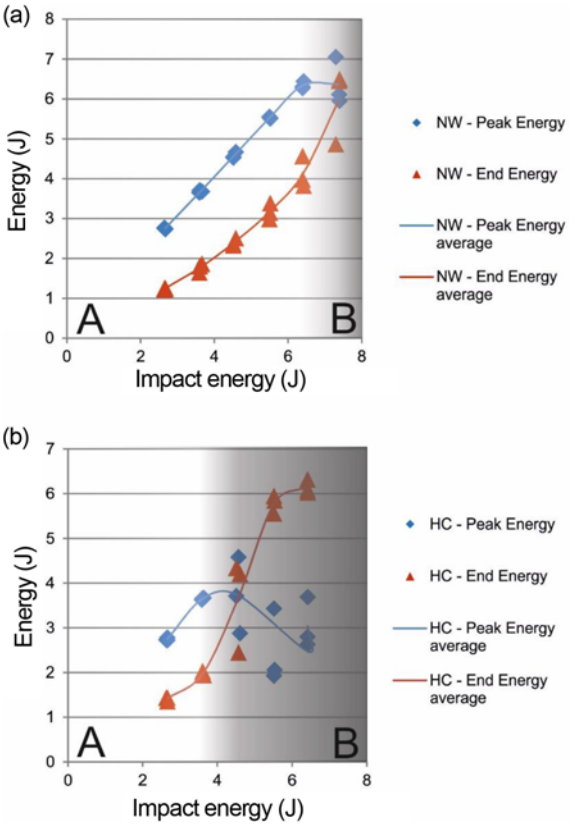

Figure 8. (a) Energy levels for peak energy and end energy in dependency of impact energy of napcore sandwiches and (b) energy levels for peak energy and end energy in dependency of impact energy of honeycomb sandwiches.

higher impact loads before the top layer gets ruptured. Table 3 and 4 list peak energy and end energy for the samples of the impact tests.

It is remarkable that the peak energy is significantly lower for the samples with ruptured face sheets compared to the dented samples. Figure 8 shows peak and end energy vs. impact energy for the tested honeycomb- and napcore-sandwich panels.

In Figure 8(a) peak and end energies for all impact tests are shown for napcore sandwiches. The peak energy increases linearly with the impact energy as long as the top layer doesn't break. All points in the light colored area represent failure mode A where the peak energy is higher than the end energy. Points in the dark colored area represent failure mode B. The difference between both energy levels equates roughly the elastic deformation of the structure. With higher impact loads the failure mode changes and at pre-set impact loads of 8 J two of three samples failed with ruptured top layers corresponding to the transition to failure mode B as defined above.

The energy levels of the honeycomb samples in Figure 8(b) show a similar behavior but the top layers get ruptured at significantly lower impact loads. As can be seen, the transition from failure mode A to B occurs around 5 J in case of the honeycomb and around 8 J for the napcore samples. With 5 J impact load two of three honeycomb-samples failed, exhibiting a ruptured top layer. At 6 J and 7 J all samples failed in mode B.

For both core materials the peak energies vary in a wide range when the face sheet gets ruptured, whereas there is only a very small variance when the face sheet doesn't break. A possible explanation for the great variance is the higher speed of the impactor at elevated loads. Exceeding a certain deformation speed, the failure of the face sheet is probably not ductile but brittle, which means the sandwich fails at lower peak energies. At the same time the peak energies show a high scattering which is a typical phenomenon for brittle failure. The damaged face sheets for failure mode A and B are shown in Figure 9.

The surfaces of the sandwich panels after impact, scanned with the 3D-scanner are shown in Figures 10 to 14. To illustrate the deformation of the top face sheet a plane was fitted to the highest points of the surface. Points close to this plane are colored green and change color with increasing distance corresponding to the topography. The areas with maximum displacement are tagged. The coloration of the bottom face sheet is similar but the plane is fitted to the lowest points of the surface.

As can be seen in Figure 2 the face sheets of napcore sandwiches are supported by aligned rows of naps. Between two adjacent rows deformation of the face sheet is alleviated which results in the two damage lines where the face sheets had failed in a bending mode as seen in Figure 9(a). The lines cross at the impact point almost but not exact rectangular.

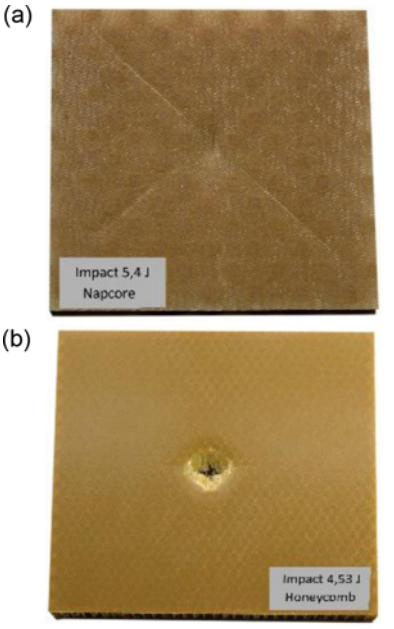

Figure 9. (a) Napcore sandwich with dented top layer after impact (Impact energy: 5.4 J) and (b) honeycomb sandwich with ruptured top layer after impact (Impact energy: 4.53 J).

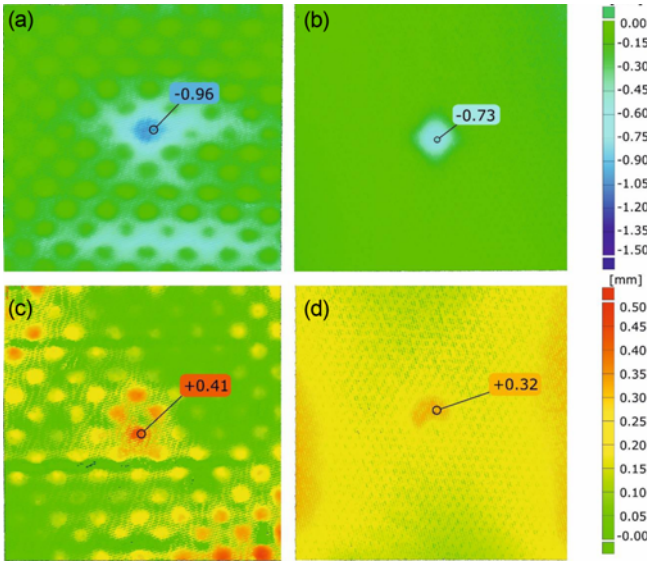

Figure 10. 3D-scan of the sandwich surfaces. Colors correspond to the topography of the surface. Tags show maximum displacement; (a) top face sheet of napcore sandwich after impact (Impact energy: 2.65 J), (b) top face sheet of honeycomb sandwich after impact (Pre-set impact energy: 2.67 J), (c) bottom face sheet of napcore sandwich after impact (Impact energy: 2.65 J), and (d) bottom face sheet of honeycomb sandwich after impact (Pre-set impact energy: 2.67 J).

The punctured top layer of the honeycomb sandwich after 4.53 J impact can be seen in Figure 9(b), In contrast the napcore sandwiches exhibit only a dented surface even at the

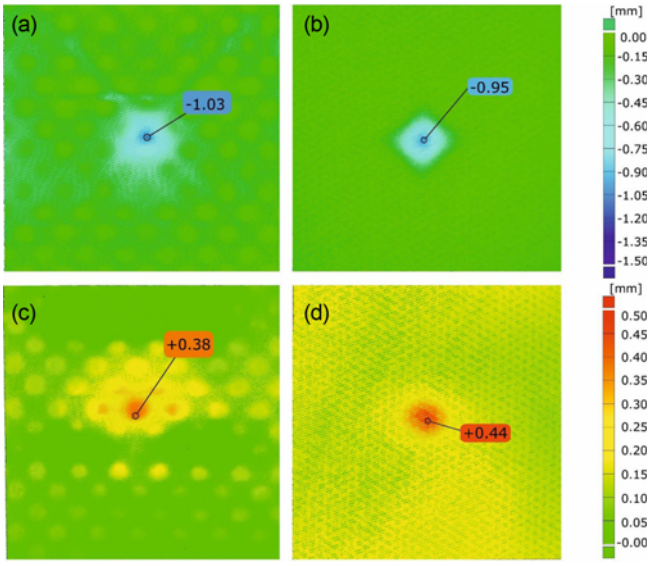

Figure 11. 3D-scan of the sandwich surfaces. Colors correspond to the topography of the surface. Tags show maximum displacement; (a) top face sheet of napcore sandwich after impact (Impact energy: 3.67 J), (b) top face sheet of honeycomb sandwich after impact (Impact energy: 3.64 J), (c) bottom face sheet of napcore sandwich after impact (Impact energy: 3.67 J), and (d) bottom face sheet of honeycomb sandwich after impact (Impact energy: 3.64 J).

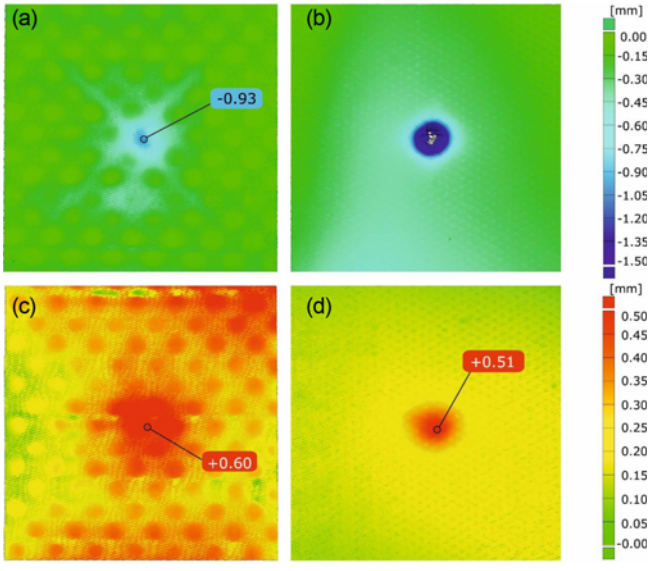

Figure 12. 3D-scan of the sandwich surfaces. Colors correspond to the topography of the surface. Tags show maximum displacement; (a) top face sheet of napcore sandwich after impact (Impact energy: 4.52 J), (b) top face sheet of honeycomb sandwich after impact (Impact energy: 4.51 J), (c) bottom face sheet of napcore sandwich after impact (Impact energy: 4.52 J), and (d) bottom face sheet of honeycomb sandwich after impact (Impact energy: 4.51 J).

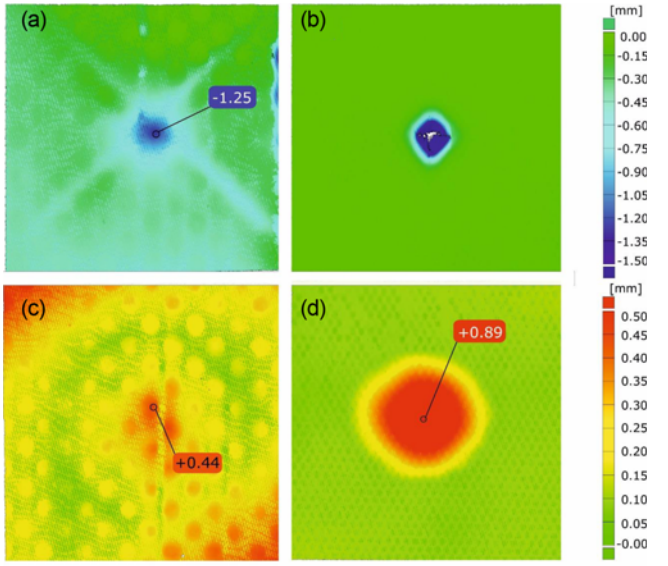

Figure 13. 3D-scan of the sandwich surfaces. Colors correspond to the topography of the surface. Tags show maximum displacement; (a) top face sheet of napcore sandwich after impact (Impact energy: 5.52 J), (b) top face sheet of honeycomb sandwich after impact (Impact energy: 5.54 J), (c) bottom face sheet of napcore sandwich after impact (Impact energy: 5.52 J), and (d) bottom face sheet of honeycomb sandwich after impact (Impact energy: 5.54 J).

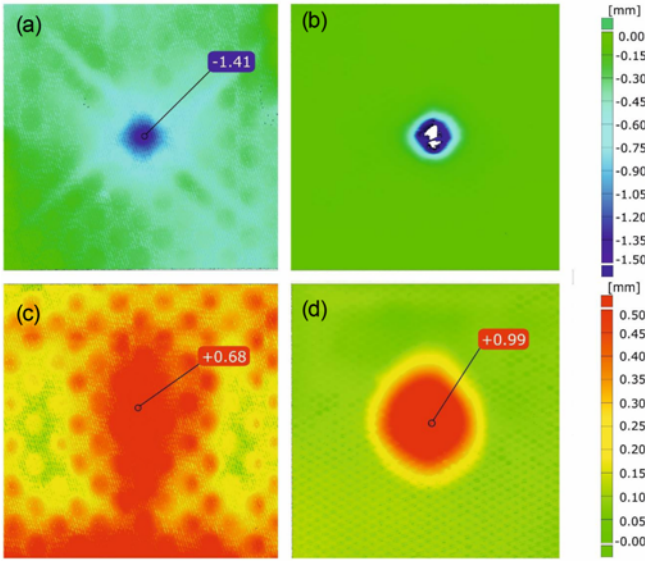

Figure 14. 3D-scan of the sandwich surfaces. Colors correspond to the topography of the surface. Tags show maximum displacement; (a) top face sheet of napcore sandwich after impact (Impact energy: 6.43 J), (b) top face sheet of honeycomb sandwich after impact (Impact energy: 6.43 J), (c) bottom face sheet of napcore sandwich after impact (Impact energy: 6.43 J), and (d) bottom face sheet of honeycomb sandwich after impact (Impact energy: 6.43 J).

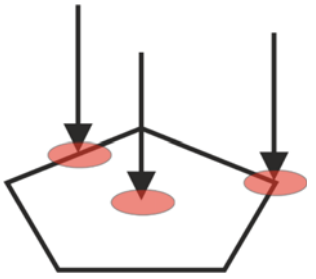

Figure 15. Three possible impact cases.

higher impact load of 5.4 J (Figure 9(a)). Since the face sheets of the honeycomb sandwiches are supported by the hexagonal cells bonded to them, the dissipation of impact load is lower than for the napcore structure. Consequently, the damage is much more local for the honeycomb sandwiches, whose surface is visually unaffected already at a short distance apart from the impact zone as can be seen in Figure 9(b). Depending on the exact impact position a slightly different damage pattern can be expected depending on the exact position where the impactor hits the honeycomb sandwich - e.g. wall or center of a cell (see Figure 15). This is likely to be one of the reasons for the higher scattering of the peak energies in case of honeycomb sandwiches.

Conclusion

Honeycomb and napcore sandwiches were analyzed under impact loads between 3 J and 8 J. The honeycomb sandwiches exhibited a stiffer behavior and the measured displacement of the sandwich surface under comparable impact energies was significantly lower than for the napcore sandwiches as long as the top layer didn't get ruptured, which was the case for pre-set impact energies below 5 J. Above 5 J the top layers of the honeycomb samples were ruptured and the deformation of the panel was irreversible. In contrast the napcore samples tolerated impact energies up to 8 J without a rupture of the top layer. Due to the napcore structure and the bonding of core and face sheets in circular areas, the impact energy is dissipated over a larger panel area, combined with a residual elastic response. This characteristic might bring napcore sandwiches in favorable position for lightweight panels with good tolerance to punctual impact loads, for example in cargo containers.

An instrumented impactor which measures both load and displacement during the impact was demonstrated to be a useful tool to distinguish between the two principle modes of impact failure observed for the two different sandwich types. Sandwiches failing with mode A show residual elasticity whereas the materials failing with mode B react fully plastic.

Acknowledgement

The authors wish to thank the Technical University of Applied Sciences in Wildau for providing the surface scanning and analyzing equipment.

References

1. N. Ischdonat, C. Dreyer, M. Bauer, and W. Gleine, Proc. 5th Inter. Workshop Aircraft Sys. Technol., 325 (2015).
2. S. Heimbs, P. Middendorf, and M. Maier, Proc. 9th Euro. LS-DYNA® Users Conf., 20 (2006).
3. T. Bitzer, "Honeycomb Technology - Materials Design, Manufacturing and Testing", 1st ed., pp.3-9, Chapman and Hall, London, 1997.
4. G. Epstein and S. Ruth, Aerospace Report No. TR-93(3904)-1, 1993.
5. V. Vavilov, A. Klimov, D. Nesteruk, and V. Shiryaev, *Proc. of SPIE*, **5073**, 345 (2003).
6. N. Gerber, M. Bauer, and C. Dreyer, *Konstruktion-Zeitschr. für Produktentw. und Ing.-Werkst.,* **3**, IW14 (2015).
7. D. G. Keith, *CA Patent*, CA1016716 (1977).
8. D. Disselbeck and D. Stahl, *U. S. Patent,* 4631221 (1986).
9. M. Bauer and C. Uhlig, *GER Patent*, DE102004062264 (2006).
10. A. Bernaschek, *Compos. Solut*., **1**, 12 (2012).
11. A. Bernaschek, Y. Chowdhury, and O. Kahle, *Proc. 2nd Inter. Conf. Thermosets*, 195 (2011).
12. M. Bauer, P. Friede, and C. Uhlig, *Kunststoffe*, **8**, 95 (2006).
13. P. O. Sjöblom, J. T. Hartness, and T. M. Cordell, *J. Compos. Mater*., **22**, 30 (1988).
14. W. J. Cantwell and J. Morton, *Composites*, **22**, 347 (1991).
15. P. M. Schubel, J. J. Luo, and I. M. Daniel, *Compos. Pt. A-Appl. Sci. Manuf*., **36**, 1389 (2005).